Investigation of Physical Properties and Thi Performance of Choline Chloride Based Deep Eutectic Solvent Using Meg as Synergetic Compound in Gas Hydrate Formation

[1]Madueke, Chimezie Stanley., [2]Osokogwu, Uche., [3]Amieibibama, Joseph

[1,2]Petroleum Engineering Department, University of Port Harcourt, Nigeria

[3]Petroleum Engineering Department, Institute of Petroleum and Energy Studies

***Corresponding author**

DOI: https://dx.doi.org/10.51244/IJRSI.2025.1210000216

Received: 20 October 2025; Accepted: 28 October 2025; Published: 15 November 2025

ABSTRACT

Flow assurance issues posed by gas hydrate to the oil industry is enormous causing economic loss, downtime and flow line blockage. However, the use of inhibitors helps to prevent hydrate formation. This work studied the synergy between (ChCl/Urea), (ChCl/Glycerol) in 1:2 molar ratios and ethylene glycol in a horizontal flow loop at constant volume condition using compress natural gas as hydrate former and the physical properties (pH, Conductivity and Turbidity) of the effluent were studied. A drop in pressure indicated that gas was used up in forming hydrate cages. The result showed that DES of sample A with MEG as synergy in 1:1 molar ratio performed better than all the five inhibitors studied. This was observed by lesser pressure decline in the loop. FTIR analysis indicated that hydroxyl group (O-H stretch), Amine or Amide group (N-H bend) and carbonyl group (C=O stretch) were the dominant functional group present in the sample and exhibited an inhibitive/bonding effect in caging and preventing the hydrogen bond from host water from encapsulating and forming hydrate in the presence of gaseous molecules. Sample B outperformed Sample A. However, the synergy of Sample A with ethylene glycol performed better than sample B with ethylene glycol. The research work is applicable in the oil and gas industry for minimizing cost and reducing toxicity of commercial inhibitors.

Keywords: Gas hydrate formation; Thermodynamic Inhibitors; Deep Eutectic Solvent; Choline Chloride; Ethylene glycol; Ionic liquid.

INTRODUCTION

Natural gas hydrates are crystalline compounds of hydrogen bonded water lattice which engulfs sized compounds like methane and carbon (iv) oxide gas at high pressure and lower temperature. It contains as much as 180-unit volume of gas at standard temperature and pressure (STP) per volume of methane hydrate. (Sloan et al., 2007). It poses serious production challenges especially with offshore exploration in deeper wells, leading to more work for production enhancement. Hydrate plug, low efficiency of hydrate dissociation and short production time in hydrate exploitation process has hindered the commercial availability of gas hydrate extraction (Shen et al., 2024). Three conditions are necessary for hydrate to be form and they are: Hydrate formation temperature and pressure usually low temperature and high pressure, presence of hydrate former e.g. methane, ethane and carbon(iv) oxide and appreciable amount of water. (Abdulmutallib et al., 2022). Growth rate and nucleation are of great importance in the process of gas hydrate formation. Nucleation can also be referred as the transition from an unstable gas-liquid phase over to a stable growth phase while Induction time is a time for the first gas-liquid contact to the first detection of hydrate phase and it is needed to predict the nucleation period. There are various options to prevent hydrate crystallization. These options include heating, insulation, water removal, and the use of thermodynamic hydrate inhibitors. THI's are used to prohibit formation of hydrates in pipelines and help in plug remediation (Odutola et al., 2022). Methanol and glycol are the most common TI's because of its low cost. However, gas regeneration and environmental issue poses extra cost.

ISSN No. 2321-2705 | DOI: 10.51244/IJRSI |Volume XII Issue X October 2025

Deep eutectic solvents (DESs) are systems formed from a eutectic mixture of Lewis or Brønsted acids and bases which can contain a variety of anionic and/or cationic species. They are partly different from ionic liquid which are formed from systems composed primarily of one type of discrete anion and cation although the physical properties of DESs are similar to other ILs, their chemical properties suggest application areas which are significantly different (Barik et al., 2022).. Generally, DESs are known for a very large depression of freezing point and are liquid at temperatures lower than 150^{o}C. However, most of them are liquid between room temperature and 70^{o}C. In most cases, a DES can be obtained by mixing a quaternary ammonium salt hydrogen Bond Acceptor (HBA) with metal salts or a hydrogen bond donor (HBD) that has the ability to form a complex with the halide anion of the quaternary ammonium salt (Abbot et. al., 2004). They are made up of large asymmetrical ions with low lattice energy, giving it a low melting point.

The oil and gas industry use different inhibitors to inhibit hydrate such as alcohols where high alcohol concentration is required to thermodynamically inhibit a gas hydrate and to shift the hydrate thermodynamic equilibrium curve to a lower temperature and higher pressure region (Najibi et al., 2022; Lu et al., 2022). 10–20 percent methanol is often used in deep water operations to prevent hydrate development in the pipelines (Abdulmutallib et al., 2022). The rate of methanol injection depends on the water cuts and inhibitor dosage. In brief, the inhibitory injection rate is obtained by multiplying the methanol dosage by the water generation rate. The inhibitory effects of ethylene glycol, ethylene glycol + PVP, and Ethylene glycol + PVP + NaCl on methane hydrate formation was studied by (Shen et al., 2025) and the influence of various temperatures, production pressure, inhibitors combination and injection time on methane hydrate dissociation was also examined. The author observed that a concentration of 30% ethylene glycol exhibits good synthetic inhibition. However, higher concentrations of both ethylene glycol and PVP in synergetic combination do not necessarily lead to better synthesis inhibition. KHIs (LDHIs) has also been used but they do not prohibit hydrate formation or alter thermodynamics but rather postpone them by decreasing the rate of hydrate formation. A KHI concentration as low as 1% can successfully stop the growth of crystals or nucleation. LDHI includes KHIs and anti-agglomerant (AAs) categories and they are characterized by having low molecular weight polymers that are dispersed in a solvent (Kelland et al., 2024). Ionic liquid and amino acid has also been used as a THIs. (Masri and Sulaimon., 2022) developed three amino acid-based ionic liquids (AAILs), 1-ethyl-3-methyl-imidazolium-glutamate (EMIMGlu), 1-(3-cyanopropyl)-3-methyl-imidazolium-glutamate (CPMIMGlu), and 1-butyl-3-methyl-imidazolium-glutamate (BMIMGlu) and studied their thermodynamic inhibition performance on methane hydrate. (Qinze et al, 2025) Investigated the effects of hydrate inhibitors on the decomposition kinetics of hydrates and elucidated their influencing mechanisms by calculating the consumption of methane, they quantified that the total methane consumption, the hydrate formation rate, the methane conversion rate, and the methane recovery rate are influenced by inhibitor types and concentrations and a determinant factor in hydrate stability. (Barik et al., 2022; Omar et al., 2022; Lomba et al., 2023; Mero et al., 2023) in different research studied the differences in the behavior of deep eutectic solvents (DESs) and room temperature ionic liquids (RTILs) in terms of their structure, dynamics, and intramolecular interactions and some of the physical properties of different DES studied were listed in table 1. (Sulaiman et al., 2024) in his work formulated a DESs that worked both as kinetic and thermodynamic inhibitor and postulated that DESs of ChCl-glycol performed better than the DESs of ChCl-glycerol.

In recent years, research has focused on deep eutectic solvent since they are environmentally safe, cost effective, easy to prepare and due to the current limitations on the use of conventional inhibitors like methanol and glycol, there is need to develop a green suitable inhibitor and DESs being an environmental friendly inhibitor is being researched. This work considers the use of Choline chloride-urea and choline chloride glycerol in 1:2 molar ratios and a conventional inhibitor as synergy in different molar ratio in varying weight percentage of 1wt%-5wt% so as to make flow assurance inhibitors eco-friendlier and highly effective. The use of FTIR was used to attribute some reasons elucidated to performance of hydrate using the presence of predominant functional groups. The physical properties (Turbidity, pH and conductivity) of solutions was studied and compared to MEG

Table 1 Physical properties of DES (Barik et al., 2022; Sulaiman et al., 2024)

Halide Salt	HBD	Viscosity/(cp)	Conductivity (mS Cm^{-1})	Density (g Cm^{-3})	Surface tension (mN m^{-1})	Molar ratio (Mp in ^{o}C ratio /final mp in^{o}C)

ISSN No. 2321-2705 | DOI: 10.51244/IJRSI |Volume XII Issue X October 2025

ChCl	Urea	632	0.75	1.24	52	1:2(303:134/12)
ChCl	Glycerol	376	1.05	1.18	55.8	1:2 (303:18/ -40)

MATERIALS AND METHODS

Deep Eutectic solvent was prepared by the addition of choline chloride + urea, and choline chloride + glycerol both chemicals were obtained from Lobachemie Chemical Manufacturers India. The mixture was prepared in 1:2 Molar ratio respectively and the eutectic mixture was heated at 60^{o}C in a water bath so that the resulting mixture becomes liquid at room temperature with a melting point of 12^{o}C and -40^{o}C respectively. Ethylene glycol (melting point of -12.9^{o}C) obtained from Molychem India was added to DES in different molar ratio to obtain the synergetic compound.

A horizontal constant volume gas hydrate flow loop mimicking a typical offshore gas pipeline that is exposed to a low temperature environment that can lead to the production of gas hydrates will be used for this experiment as shown in figure 1 and instrument functions and ranges shown in table 2. The hydrate loop is made of 316 stainless steel tubing of 0.5-inch internal diameter and 12 meters long. This steel tubing is concentrically encased in a 4-inch polyvinylchloride (PVC) pipe, which is kept cool by regular water circulation. The PVC pipe is insulated to avoid heat gain or loss from the system.

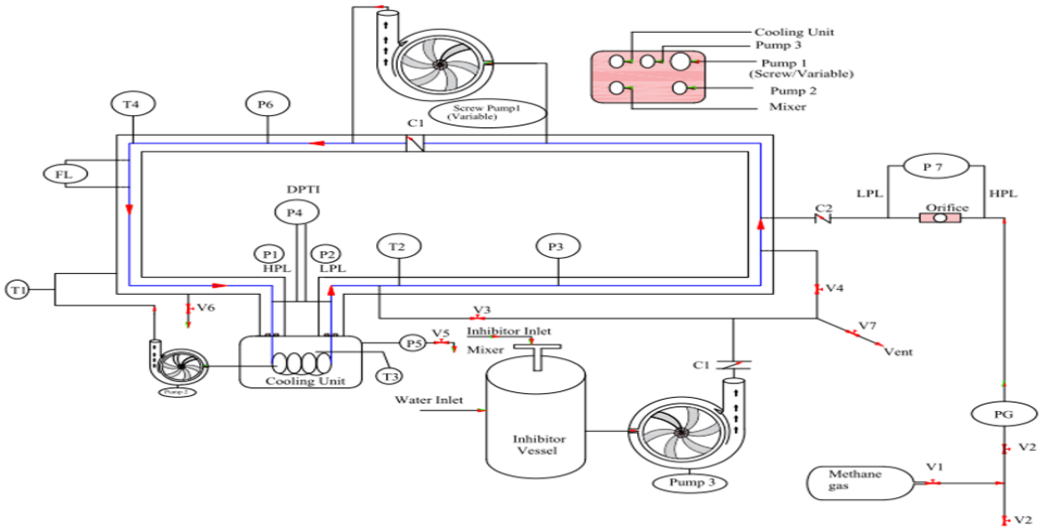

Figure 1 A Sketch of experimental hydrate flow loop

The experimental investigation of gas hydrate prevention using inhibitors was performed at same operating condition of the flow loop. After the preliminary preparation, 2600ml (100%) of water was measured and turned into the inhibitor vessel. Valve 5 and pump 3 were then turned on to build up pressure up to 25 psi and thereafter, valve 5 and pump 3 were turn off. The compressed natural gas (CNG) was injected or pumped into the system by turning on valve 1, valve 3 and the orifice. The valves were turned off after attaining to the maximum operating loop pressure. Pump 2 was turned on to fill the jacket with the cooling water from the refrigerator loaded with ice and kept running until the temperature at which hydrate was formed. At every time interval of 2 minutes for a period of 2 hours, the inlet and outlet (flow loop) pressure, inlet and outlet (flow loop) temperature, cooling water (sub cooled) temperature and sample point (hydrate forming) pressure were recorded. The experiment was repeated by measuring and injecting the concentration of inhibitors investigated at 26.6ml, 79.8ml, 133ml representing 1wt%, 3wt%, 5wt%, respectively with 2573.4ml, 2520.2ml and 2467ml of water into the inhibitor vessel and allow to run.

The calculated Inhibition efficiency (IE) is given as:

IE = (1-Y) %

ISSN No. 2321-2705 | DOI: 10.51244/IJRSI |Volume XII Issue X October 2025

Where Y is the inhibition factor given as

$Y = \Delta P_{inhibited} / \Delta P_{uninhibited}$ (1)

$\Delta P_{inhibited} = P_i - P_{inhibited}$ (2)

$\Delta P_{uninhibited} = P_i - P_{uninhibited}$ (3)

Table 2 Instrument used, Functions and Ranges

Instrument	Functions	Ranges	Units
Inlet and Outlet Pressure Gauge, [P2, P1]	Pressure measurement	0-500	psi
Pressure Along the Flow loop, [P3]	Pressure measurement	0-500	psi
Outlet Point Temperature Gauge, [T1]	Temperature measurement	-50 - 50	^{0}C
Inlet Point Temperature Gauge, [T2]	Temperature measurement	0 – 100	^{0}C
QB60 Pump, [Pump 1 &2]	Circulation of fluids	0.5	hp
ATP 1.25 Pump, [Pump 3]	Circulation of fluids	1	hp
Pipe internal diameter	Distance	0.0127	m

A Hach 2100N Turbidimeter with parameters shown in Table 3 was used to measure the turbidity of the effluent while Thermo-scientific Orion Star A215 Meter comprising of pH electrode and Conductivity electrode with parameters in table 4 was used to measure the value of pH and Conductivity respectively.

Table 3 HACH 2100N Specification

Measurement method	**2100N**
NTU mode (decimal)	0-4000 (0-0.9999)
Accuracy	±2% of reading plus 0.01NTU from 0-40 NTU under reference condition
Operating temperature / sample temperature	0 to 40°C (32 to 104°F)/ 0 to 95°C (32 to 203°F)

Table 4 Thermo scientific Orion star A215 Model

Measured quantity	**Description**
pH	**Range**: -2.000 to 20.000 **Resolution**: 0.1, 0.01, 0.001 **Relative Accuracy:** ±0.002 **Calibration Points**: Up to 5
Conductivity	**Range**: 0.001 µS to 3000 mS **Resolution:** 0.001 µS minimum, auto ranging, up to 4 significant digits **Relative Accuracy**: 0.5 % of reading ±1 digit > 3 µS, 0.5 % of reading ±0.01 µS ≤ 3 µS
Inputs	**pH Electrode**: BNC, reference pin **Conductivity or ATC Probe**: 8-pin mini-DIN

Fourier Transformed Infrared Spectroscopy (FTIR) was utilized for predicting the active functional group present in the chemical inhibitor hence predicting the behavioral pattern of the inhibitor. The analysis reveals chemical bonds in a molecule by producing an infrared absorption spectrum which is useful in examining

ISSN No. 2321-2705 | DOI: 10.51244/IJRSI |Volume XII Issue X October 2025

functional groups of compounds. The Y axis in the graph denotes the %Transmittance while the X axis denotes the wavelength (cm^{-1}) and peaks in the spectrum reflect specific molecular vibrations.

RESULTS

Physical properties of Inhibitor:

After the experimental run, 1wt% and 5wt% of the effluent samples was collected and the physical properties (Turbidity, conductivity and pH) was checked at 25ºC and the result provided in Table 5 below. The pH was recorded to have a range of 6.01-6.68 for the six samples considered while the inhibitor conductivity increases as synergetic compound (MEG) is added to the DESs and this is true for all studied DESs in this work. However, the turbidity of MEG was found to be higher than the studied DESs

Table 5 Inhibitor sample and physical properties of solution after experiment run @ 25ºC

DESs Inhibitor samples	Molar ratio	Weight%	pH of solution	Conductivity mS/Cm^{-1}	Turbidity
ChCl+Urea (Sample A)	1:2	1	6.01	0.0955	3.10
		5	6.48	0.609	1.44
ChCl+Glycerol (Sample B)	1:2	1	6.02	0.0497	2.54
		5	6.42	0.0610	1.14
Sample A+ Ethylene glycol (Sample C)	1:1	1	6.23	0.632	1.352
		5	6.39	0.4263	3.37
Sample A + Ethylene glycol (Sample D)	2:1	1	6.65	0.632	0.352
		5	6.68	0.3003	0.922
Sample B + Ethylene glycol (Sample E)	1:1	1	6.26	0.0830	2.28
		5	6.35	0.0610	1.66
Ethylene Glycol (Sample F)		1	6.12	0.0220	9.47
		5	6.15	0.0521	7.68

Hydrate Profile without Inhibitor.

For the uninhibited experiment (water and gas only) as illustrated in figure 2 the initial temperature and sub cool final temperature was 32^0C and -2ºC respectively with initial pressure of 150 psi. For the first 30 minutes, the pressure drops to 120psi. After roughly an hour, the pressure dropped to 105psi. After 90 minutes, the pressure dropped to 65 psi then to 47 psi after 120 minutes. The temperature followed the same downward pattern as the pressure versus time curve thus, the influence of the sub cool temperature on the flow line causes a decrease in the operating pressure. Temperature dropped from 32^0C to 9^0C in 44 minutes, then began to rise from 9^0C to 20.5^0C at 100 minutes and finally rose to 22.5^0C by the end of 120 minutes. The spike in temperature was due to continuous dissolution of methane gas in the cooling water which caused a reduction in induction time. As hydrate began to develop, the half inch inner line began to emit heat. This was due to the fact that hydrate formation is an exothermic process (Movareji et al., 2016; Odatuwa et al., 2024). As hydrate formed in the inner line, gas was used up, resulting in a significant drop in loop pressure (Elechi et al., 2021; Odutola et al., 2022).

ISSN No. 2321-2705 | DOI: 10.51244/IJRSI |Volume XII Issue X October 2025

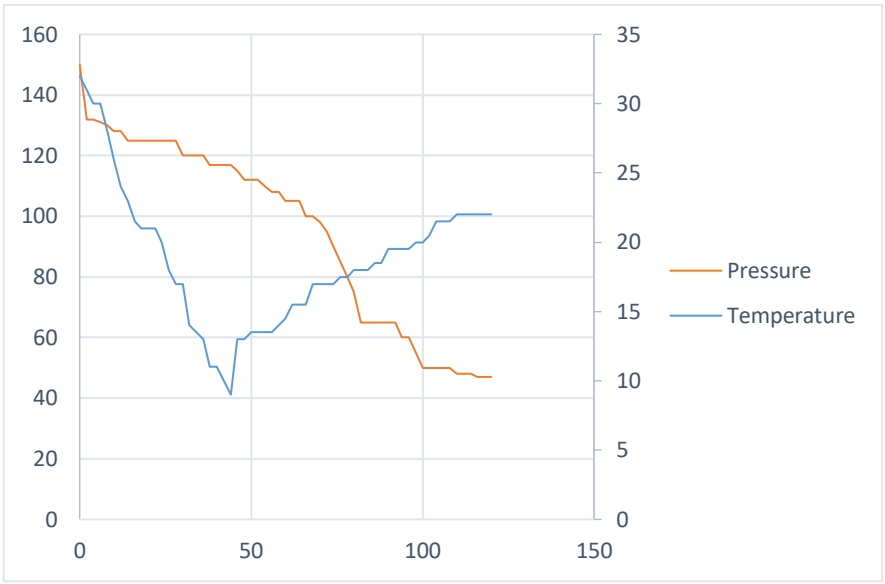

Figure 2 Pressure(psi) and Temperature ^{0}C versus time(min.) for Uninhibited experiment

Mono ethylene glycol as an Inhibitor (Sample F):

When MEG was used as an inhibitor as indicated in figure 3 and figure 4 below for sub cool temperature range of 32ºC to -2ºC gas hydrate was inhibited and from the result, it was observed that inhibitor performance was proportional to increase in concentration. Pressure dropped to 102psi, 107psi and 110psi with effluent volume of 850ml, 880ml and 910ml corresponding to 1wt%, 3wt% and 5wt% respectively at the end of the experimental run. The graph illustrates that 5wt% of MEG showed a better inhibition capacity with a calculated efficiency of 61.17% while the efficiency of 3wt% and 1wt% was 58.25% and 53.4% respectively. However, 5wt% will be regarded as the optimum wt% for this experiment since increasing the dosage significantly affected the performance of the inhibitor. The FTIR in figure 5, showed a broad peak at point 3298cm^{-1} indicating the presence of a very strong and stretched hydrogen bond. Points 2937 cm^{-1} and 2874 cm^{-1} indicated the presence of two aliphatic C-H groups. Vibrations at points 1082 cm^{-1} and 1035 cm^{-1} showed hydrogen bonding which was due to two primary alcohol attached and were influenced due to the presence of a strong =C-H bend at 1745cm^{-1}. The strong hydroxyl group was responsible for the inhibitor performance and prevented hydrogen bonding of the host water $(O\text{-}H)_w$ from encapsulating gaseous particles forming hydrate. Hence shifting the thermodynamic equilibrium towards free water and gas zone (Odatuwa et al., 2024).

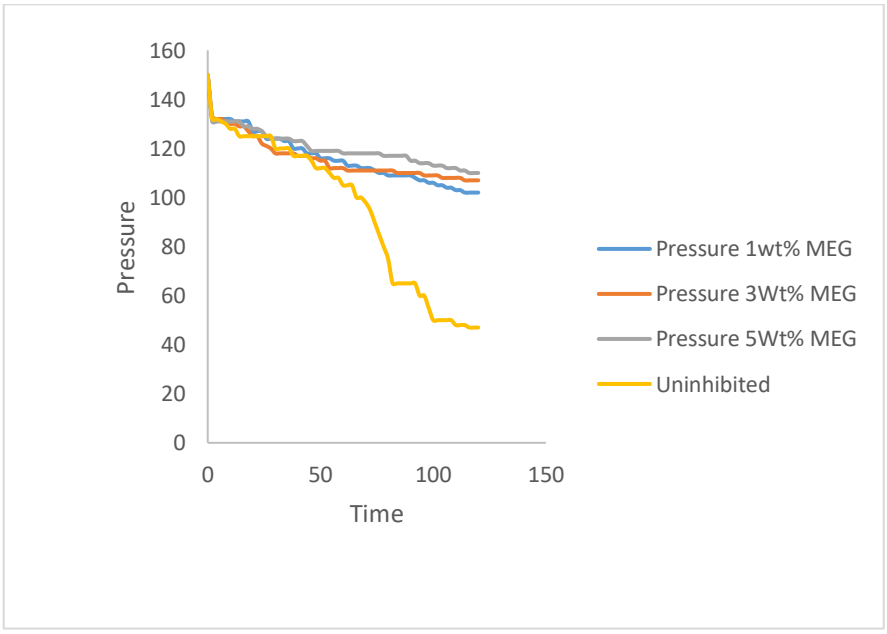

Figure 3 Pressure(psi) vs time(min) Sample F

ISSN No. 2321-2705 | DOI: 10.51244/IJRSI |Volume XII Issue X October 2025

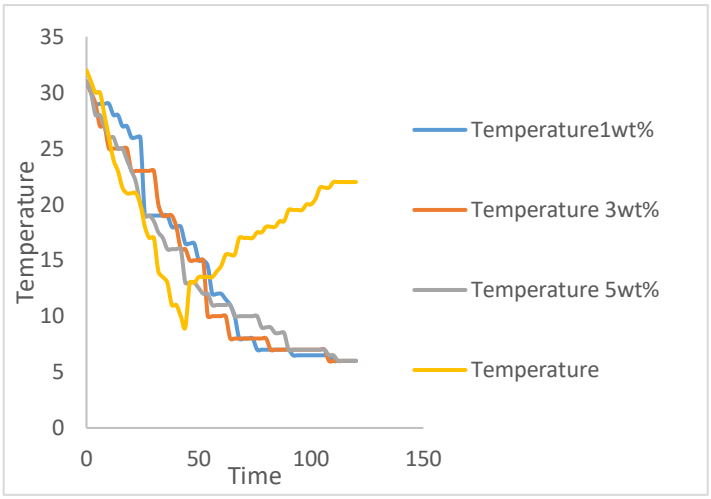

Figure 4 Temp. (^{O}C) vs Time(min) for sample F

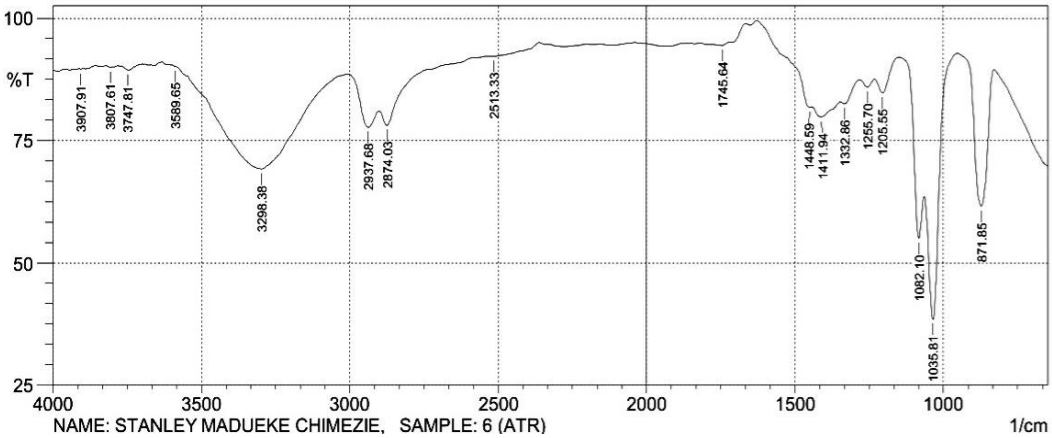

Figure 5 FTIR analysis for Sample F

Choline chloride-urea based hydrate inhibitors with its synergetic compound:

The eutectic mixture of Choline Chloride (303^{O}C MP) with Urea (134^{O}C MP) formed a solvent which is liquid at room temperature (12^{O}C MP) and when used as an inhibitor in figure 6 below, gas hydrate was inhibited and from the result, it was observed that inhibitor performance was not proportional to increase in concentration as observed also by (Madueke et. al., 2023) . The pressure dropped to 105psi, 100psi and 107 psi at subcool temperature of -2^{O}C corresponding to 1wt%, 3wt% and 5wt% respectively at the end of the experimental run. 5wt% of DES showed a better inhibition capacity with a calculated efficiency of 58.25% while the efficiency of 3wt% and 1wt% was 51.45% and 56.31% respectively

A greater synergy was observed when MEG was used in 1:1 ratio (choline chloride Urea: MEG) in sample C than in sample D (2:1 molar ratio). Sample C had pressure dropped to 116psi,122psi and 127psi at final subcool temperature of -2^{O}C by the end of the experiment corresponding to 1wt%, 3wt% and 5wt% as illustrated in figure 7 with calculated inhibitor efficiency of 66.99%, 72.8% and 77.7% corresponding to 1wt%,3wt% and 5wt% respectively and when the pressure was compared to sample D in figure 8, it was reported to be 111psi,99psi and 99psi at the end of the 120 minutes. The calculated inhibitor efficiency was 62.13%, 50.49% and 50.49% corresponding to 1wt%,3wt% and 5wt% respectively. However, sample D at 3wt% and 5wt% acted as hydrate promoter with inhibitive capacity as wt% increases. The poor performance of sample D at 3wt% and 5wt% is in line with a study carried out where inhibition greater than 1% did no offer a lot of advantages (Odutola et al., 2022).

The FTIR analysis in figure 9 for sample A indicated the presence of weak bonded (N-H) symmetric amide functional group at point 3192cm^{-1} and a strong broad hydroxyl functional group (O-H) at point 3323 cm^{-1} which were perfectly aligned from the eutectic mixture of choline chloride (O-H) and urea(N-H) and both compounds

ISSN No. 2321-2705 | DOI: 10.51244/IJRSI |Volume XII Issue X October 2025

contributing to the hydrogen bonded network thereby preventing water from mixing with methane gas as temperature decreases in the loop (Elechi et al., 2021). The carbonyl group on point around 1662 cm^{-1}- 1602 cm^{-1} (C=0) stretched vibration aided the stability and affected the formation of supplementary hydrogen bonding while preserving the distinct properties in all the choline chloride-urea and its synergistic component considered. This was supported in the research conducted by (Arkawazi et. al., 2020; Rao et. al., 2025). Point 1440 cm^{-1} depicted a CH_2 bending or scissoring from choline moiety while point 1161 cm^{-1}-1040 cm^{-1} indicated C-N and C-O from choline and urea indicating hydrogen bonding interaction. Howbeit, confirming the presence of amide and alcohol functional group. The strong performance of choline chloride urea and MEG (Sample C) in figure 10 can be attributed to strong broad peak at point 3329 cm^{-1} and 3201 cm^{-1} (O-H and N-H) stretch indicating significant hydrogen bonding which is broader and more intense when compared to sample A. However, the MEG added more HBD enhancing the hybridization. The shift to 1616 cm^{-1} in sample C when compared to sample A 1662 cm^{-1} (figure 9) showed that the carbonyl group is more involved in hydrogen bonding due to MEG's hydroxyl forming abilities. Broad and slightly perfectly merged band of C-O and C-N stretching occurred between 1332 cm^{-1} - 1163 cm^{-1} with C-O from MEG and C-N from choline. The waggling effect of C-O and C-N at point 1038 cm^{-1} contributed to very strong inhibitive performance.

The poor performance of sample D in figure 11 can be attributed to the reduction on the influence of the strong hydroxyl bond at point 3333 cm^{-1} (lesser O-H influence) and the consistent appearance of weak to moderate band N-H bond in the region of 3201 cm^{-1} and 3416 cm^{-1} when compared to sample C in figure 10, thus leading to reduction in hydrogen bond density due to higher choline chloride and urea concentration Point 1662 cm^{-1}-1614 cm^{-1} in figure 11 showed C=0 stretch which had more intensity than in sample C indicating the presence of excess urea which was less involved in hydrogen bonding while point 1165 cm^{-1}-1041 cm^{-1} in fig 10-11 showed C-O and C-N vibration and indicated that sample C which had more intensity, had more complex interactive network due to higher availability of hydroxyl group from MEG when compared to sample D and it is attributed to some reasons for the poor performance of sample D.

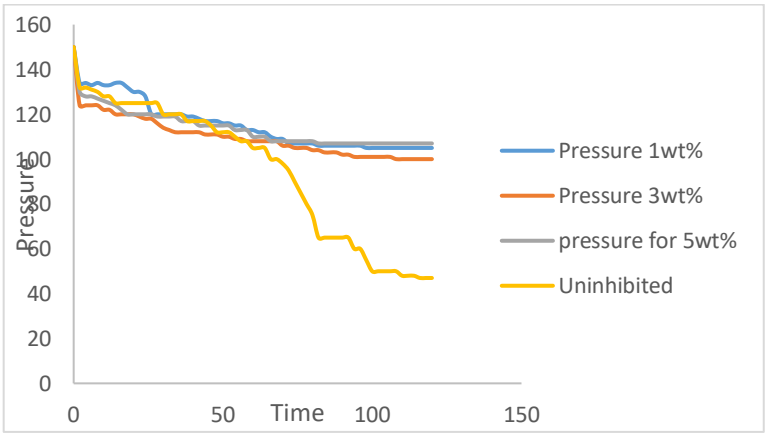

Figure 6 pressure(psi) vs time(min) Sample A

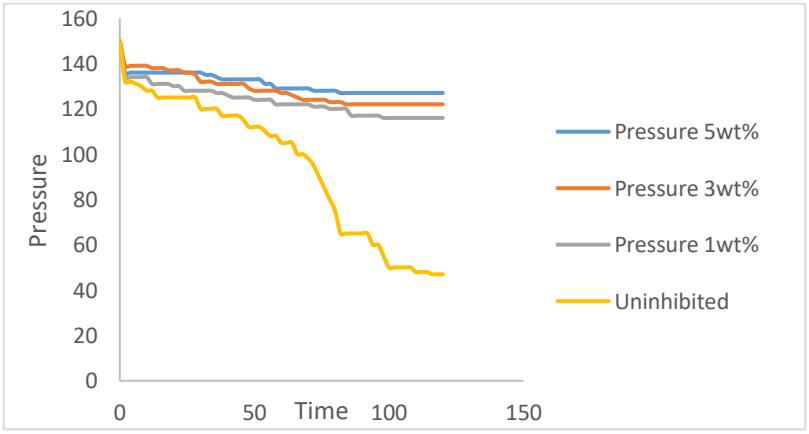

Figure 7 Pressure(psi) vs time(min) Sample C

ISSN No. 2321-2705 | DOI: 10.51244/IJRSI |Volume XII Issue X October 2025

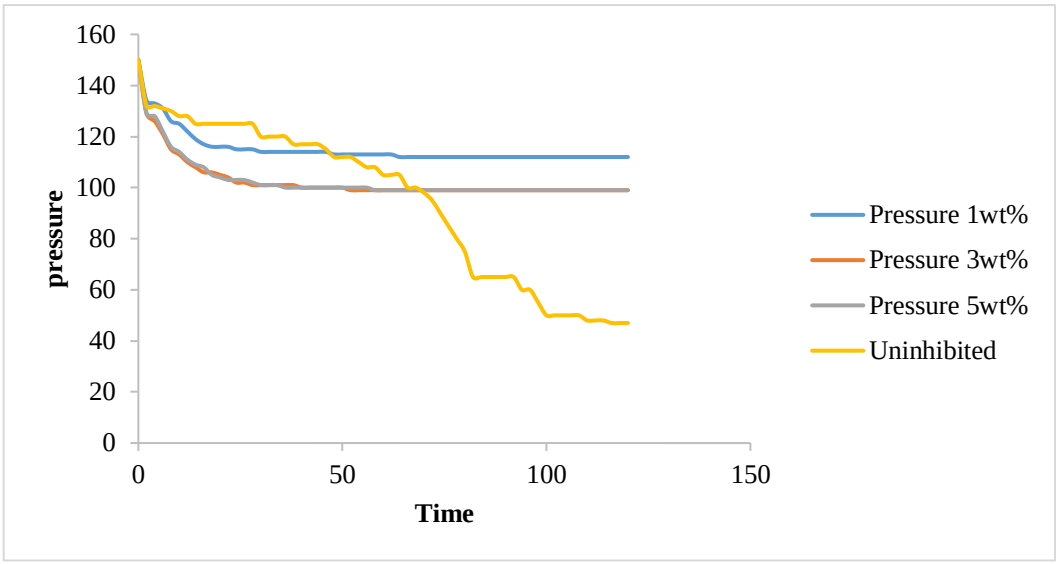

Figure 8 Pressure(psi) vs time(min) sample D

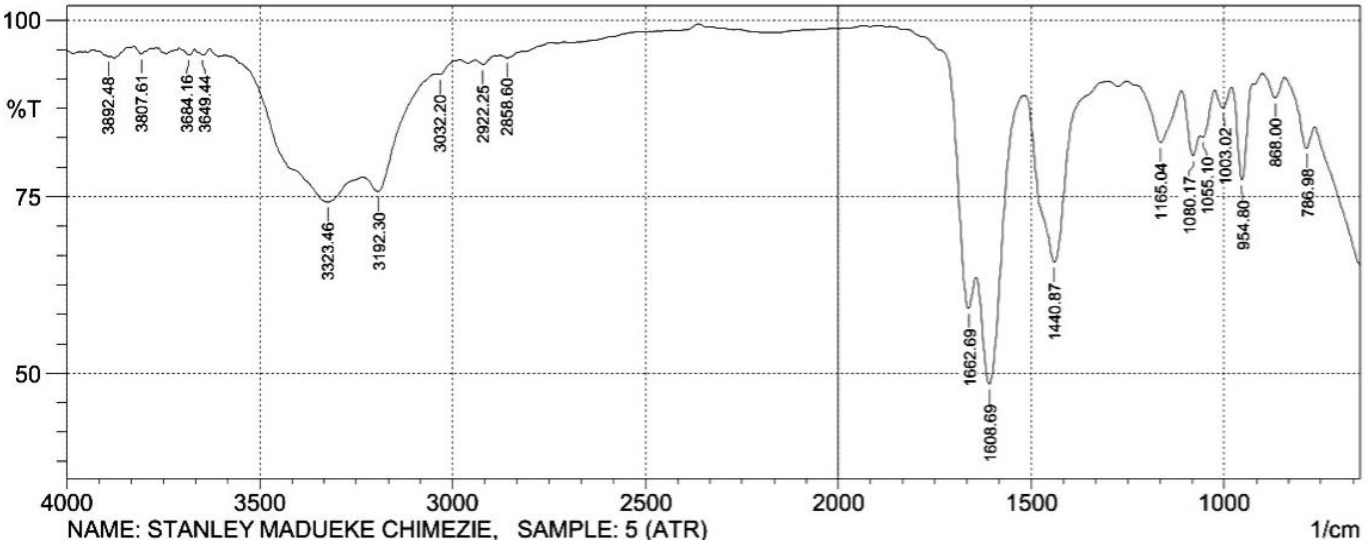

Figure 9 FTIR analysis for sample A

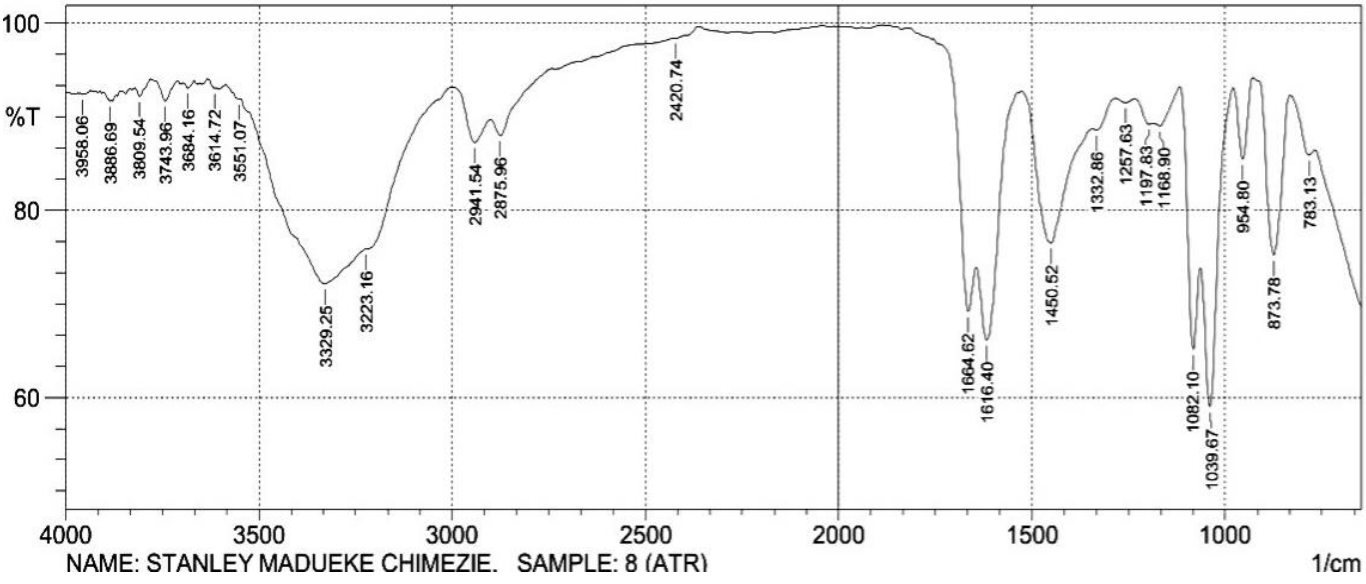

Figure 10 FTIR analysis for sample C

ISSN No. 2321-2705 | DOI: 10.51244/IJRSI |Volume XII Issue X October 2025

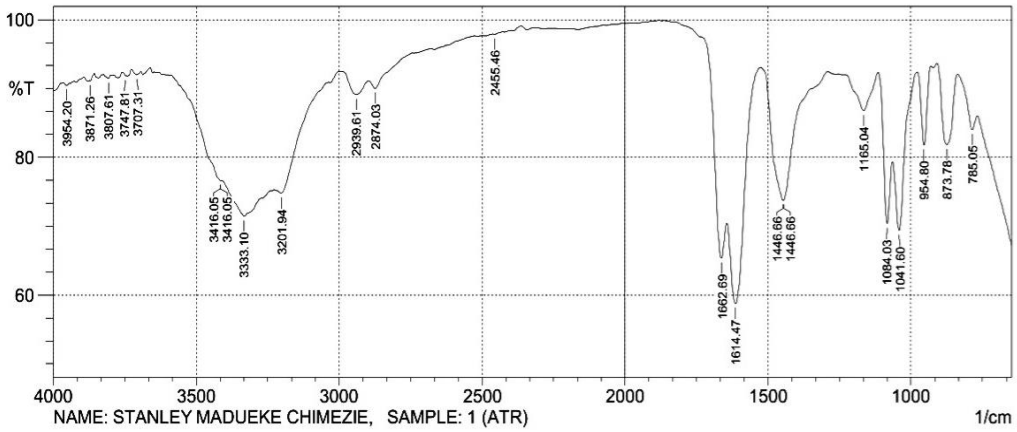

Figure 11 FTIR analysis for Sample D

Choline chloride-glycerol based hydrate inhibitors with its synergetic compound:

The eutectic mixture of Choline Chloride (303^{O}C MP) with glycerol (18^{O}C MP) in 1:2 molar ratio formed a DES solvent which is (-40^{O}C MP) and when it was used as an inhibitor as indicated in figure 12 below, gas hydrate was inhibited. However, from the result, it was observed that inhibitor performance was proportional to increase in concentration. There was pressure drop from 150psi to 104psi, 108psi and 110psi at subcool temperature of -2^{O}C whereas effluent volume of 860ml, 890ml and 900ml was collected corresponding to 1wt%, 3wt% and 5wt % respectively at the end of the experiment. 5wt% of DES showed a better inhibition capacity with a calculated efficiency of 61.17% while the efficiency of 3wt% and 1wt% was 59.22% and 55.34% respectively. However, 5wt% will be regarded as the optimum wt% for this study since increasing the dosage significantly affected the performance of the inhibitor. MEG is a poor synergy for DES comprising of Choline chloride and Glycerol. All the wt% of Choline chloride and glycerol in sample B performed better when compared with its synergy (Sample E). However, at increased wt%, The inhibition performance of sample E decreases indicating it acted more as hydrate promoter than inhibitor as concentration increases. The calculated efficiency of 51.5%, 40.8 % and 35 % for 1wt%, 3wt% and 5wt% respectively indicated that choline chloride-glycerol is not a good synergy with MEG and this was also indicated with effluent volume of 790ml, 760ml and 730ml corresponding to 1wt%, 3wt% and 5wt% respectively at the end of the experimental. However, the effect of volume of hydrate was not studied but the volume of effluent recorded at the end of every experimental run decreases as the concentration of inhibitor increases. This phenomenon shows that the higher the volume of effluent recorded the better the performances and effectiveness of inhibitor used (Nwaibu et al., 2018). During the experimental run for sample E, it was observed that gas was almost used up to form hydrate cages or crystals which was visible as it began appearing in tiny observable crystals when the effluent was collected for 3wt% and 5wt% since the influence of the sub cooling temperature of the flow line causes a decrease in the operating pressure and gas hydrate formation temperature. Figure 13 illustrates the graph of pressure versus time for sample E with a pressure drop from 150psi to 113psi, 101psi and 97psi at subcool temperature of 4^{O}C and final pressure of 100psi, 89psi and 83psi corresponding to 1wt%,3wt% and 5wt% respectively at the end of 120minutes. The poor performance of the synergetic compound in higher weight % can be attributed to the increase in molecular weight. and poor intermolecular interaction. This view was supported by (Scong et al., 2017) whose work illustrated that molecular weight affects the performance of hydrate inhibitor.

FTIR analysis in figure 14 indicated the presence of a strong hydrogen bonding stretch at peak point covered around point 3321 cm^{-1}. This was due to multiple hydroxyl group associated with glycerol aiding hydrogen bond formation. Peak point of 2930cm^{-1}-2840cm^{-1} showed an aliphatic C-H stretched vibration likely from methyl and methylene group of choline and glycerol respectively while a C-N/N-CH_3 asymmetry stretch from 1475cm^{-1}-1467cm^{-1} is related to a quaternary ammonium group ($N^{+}(CH_3)_3$) from choline chloride. C-O stretch/C-O-C vibration at point 1037cm^{-1} confirms strong interaction between choline chloride and glycerol respectively. This was supported by the peak shift and change in intensity from free glycerol conducted by (syahputra et. al., 2023) indicating strong intermolecular hydrogen bonding with choline chloride. Sample E FTIR graph in figure 15 indicated strong broad hydrogen bonding from glycerol and MEG at point 3360cm^{-1}. The aliphatic C-H stretch occurred at point 2937 cm^{-1}-2874 cm^{-1} but the presence of slightly intensed C=O stretch at point 1708 cm^{-1} likely

ISSN No. 2321-2705 | DOI: 10.51244/IJRSI |Volume XII Issue X October 2025

from oxidation of MEG into a different functional group (e.g. Aldehyde group absorption range) with strong absorption affecting the hydrogen bonding and overall inhibition performance of sample E but when compared to sample B in figure 14, it was reported to be less significant with different insignificant absorption range. the poor performance due to oxidation was supported by a study conducted by (Khalifa et. al., 2015) whose study reported that thermally degraded MEG undergo oxidation reaction and was a poor hydrate inhibitor when compared to MEG at normal condition. There was CH_2 bending / $N^+(CH_3)_3$ symmetric bend at point 1411 cm^{-1}-1255 cm^{-1}. from the choline group. Sample E possess similar characteristics to Sample B e.g. C-O stretch on point 1032 cm^{-1} which appeared on point 1082 cm^{-1}. in sample E. The slight shift is due to interaction of the hydroxyl group from MEG.

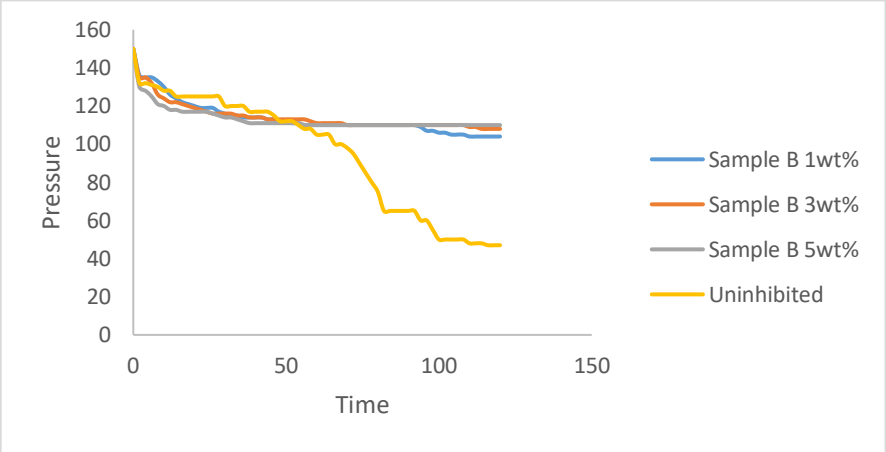

Figure 12 Pressure(psi) vs time(min)Sample B

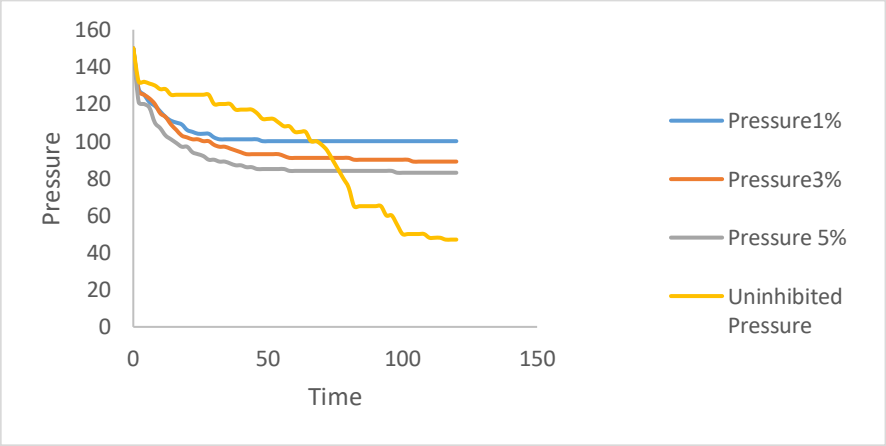

Figure 13 Pressure(psi) vs time(min) sample D

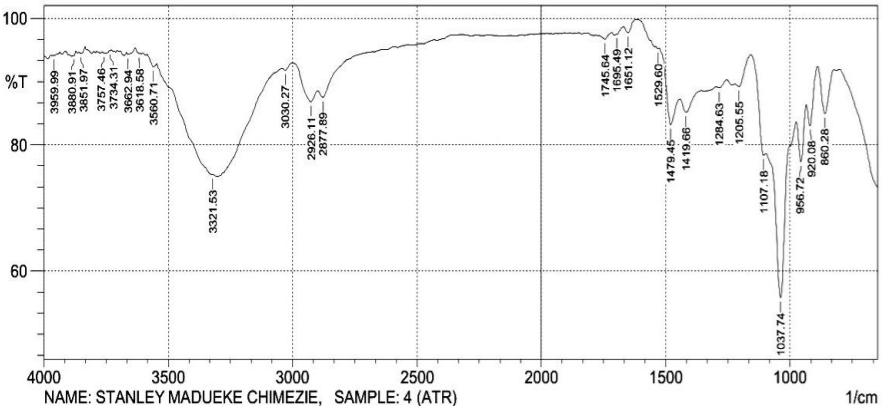

Figure 14 FTIR analysis for sample B

ISSN No. 2321-2705 | DOI: 10.51244/IJRSI |Volume XII Issue X October 2025

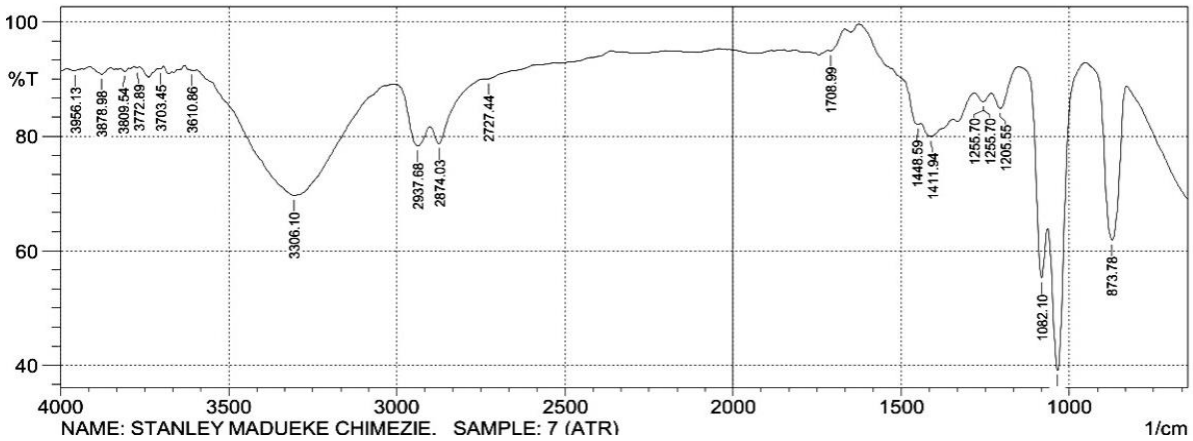

Figure 15 FTIR analysis for sample E

Temperature profile with DES inhibitor and without Inhibitor:

It was observed from figure 16, that loop temperature decreased uniformly when inhibitors was used indicating that the inhibitors were successful in preventing hydrate formation which is accompanied by an increase in temperature. However, there was hydrate formation when no inhibitors were used, this can be observed by the sudden increase in loop temperature at 58 minutes from 13.5^{o}C to 14^{o}C and at the end of the 120 minutes, the temperature rose to 22^{o}C.

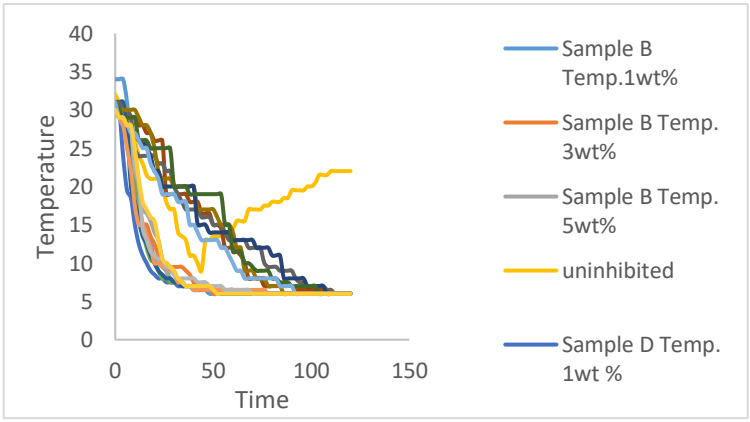

Figure 16 Temp. (^{O}C) vs Time(min) for DES samples considered

DISCUSSION

From the experimented result, The five DESs and MEG considered were able to inhibit hydrate at different weight percentage of 1wt %, 3wt% and 5wt% and acted by altering water molecules $(O\text{-}H)_w$ with the strong (O-H)a and weak to medium (N-H) bond making it unfavorable for hydrate formation to occur while pushing the equilibrium position towards a hydrate free zone. However, Sample D and sample E acted as a hydrate promoter in higher weight percentage since increasing the inhibitor weight percentage reduces the hydrate inhibition performance indicating that ethylene glycol is not a good synergetic compound for choline chloride- urea based DES in 2:1 ratio (sample D) likely due to excess urea which was less involved in hydrogen bonding and Choline-glycerol based DES in 1:1 molar ratio (sample E). This was similar to the result gotten by (Odutola et al., 2022) when PVP was used as a synergy in a thermodynamic under inhibited system. More research will be needed to determine the molar ratio for effective synergy for choline chloride-glycerol based DES in the future since oxidation of MEG in sample E played an important role in hydrogen bond linkage (Khalifa et. al., 2015). The synergetic effect of Choline Chloride-urea and ethylene glycol in 1:1 ratio (sample C) performed better and was able to inhibit hydrate formation more effectively. This can be observed with the volume of effluent of 980ml,1040ml and 1080ml at the end of the experiment and the inhibitor efficiency of 66.99%, 72.8% and 77.7% corresponding to 1wt%, 3wt% and 5wt% respectively. The higher the volume of effluent, the greater the inhibitor efficiency in preventing the gas engulfed by water molecules forming hydrate (Nwaibu et al., 2018). From the

ISSN No. 2321-2705 | DOI: 10.51244/IJRSI |Volume XII Issue X October 2025

FTIR result in figure 10, the performance of sample C can be attributed to the increase surface area of the strong hydrogen bond (O-H)a and its successive effect in interacting with water molecules. The conventional inhibitor ethylene glycol is used to compare and validate the performance of each DES inhibitor and it was observed that ethylene glycol performed slightly better than sample A, while sample B performed better than ethylene glycol (sample F) in 1wt% and 3wt% but as wt% increases, the calculated inhibition efficiency of ethylene glycol increases surpassing sample B. Graph of figure 17 and figure 18 represent the calculated inhibitor efficiency of the 6 samples considered and the pressure drop (P_f-P_i) in relation to time respectively. The figures showed that 1wt%, 3wt% and 5wt% of sample C performed more than all the inhibitors considered when studied individually and the experiment without inhibitor (uninhibited) had the highest pressure drop with a value of 103psi. However, 5wt% is the optimum dosage for sample C. Moreover, 1 wt% of Sample C performed better than all wt% of MEG considered, therefore the addition of sample C will greatly reduce the percentage of MEG needed in the industry for hydrate inhibition and overall cost associated with MEG regeneration.

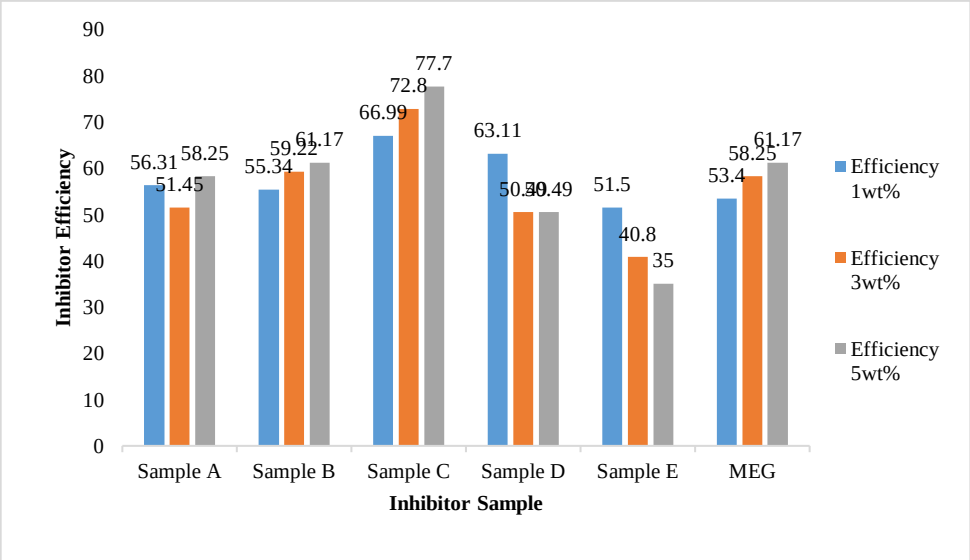

Figure 17 Inhibition Efficiency of Samples

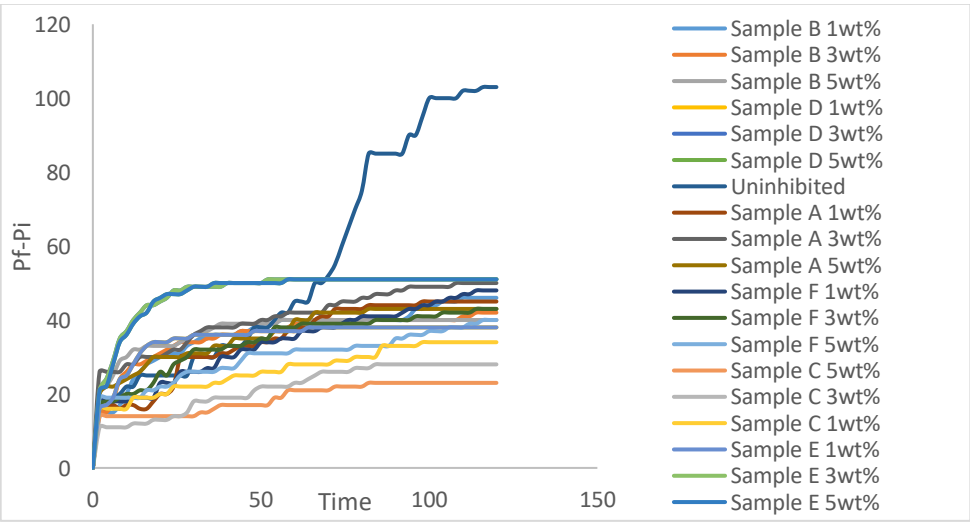

Figure 18 Differential pressure drop (P_f-Pi) (Psi) vs time(min)

CONCLUSION

This work investigated the inhibitive performance of choline chloride based deep eutectic solvents using MEG as synergetic compound on a constant volume flow loop mimicking an offshore transport line. Various inhibitors were validated and compared with the Conventional MEG. The physical properties of the inhibitors were determined at 25^{o}C. The pH was recorded to have a range of 6.01-6.68 for the six samples considered while the

inhibitor conductivity increases as synergetic compound (MEG) was added to the DESs. Turbidity of MEG was found to be higher than the studied DESs. FTIR was used to predict the active functional group, bond interaction and behavior of DES properties present in the mixture. The poor performance of Sample D is likely due to excess urea which was less involved in hydrogen bonding while the oxidation of MEG into a different functional group in Aldehyde absorption range affected the hydrogen bonding and overall inhibition performance of sample E. This research work will be recommended for field trial since sample C will reduce the toxicity and wt% of MEG required for hydrate inhibition. 1 wt% of sample C synergy performed better than 5wt% of MEG (sample F). However, the cost associated with regeneration of MEG will be greatly reduced since all DESs considered with the exception of sample E altered only the physical interaction while the chemical morphology of each component remained intact with little shift, bend or waggling (Juric et. al., 2021). Hence no new product was formed as illustrated from the FTIR results.

Ethics declarations

The authors declare no conflict of interest and all authors agreed and approved the manuscript

ACKNOWLEDGEMENT

I am grateful for God for giving me the strength and knowledge to compute this article and to my dear wife for her support. A special Thanks to my HOD Petroleum Engineering Dr. Osokogwu Uche and the assistance director for Institute for petroleum Studies Associate Prof. Amieibibama, Joseph for their supervision, guidance and support.

Grants and Funds

The author declares that there are no grants and funds received during the preparation of this manuscript

Statement and Declaration

The authors declare that they all contributed to this manuscript and they all read and approved the final manuscript

REFERENCE

1. Abbott, A. P.; Boothby, D., Capper, G., Davies, D. L. (2004). Deep Eutectic Solvents Formed Between Choline Chloride and Carboxylic Acids: Versatile Alternatives to Ionic Liquids. J. Am. Chem. Soc. 126, 9142−9147
2. Abdulmutalib, A., & Abdulmalik, F. (2022). Investigation of hydrate formation in natural gas transmission pipelines. International Journal of Advance in Engineering and Management. 4(5), 2040-2055 https://doi.org 10.35629/5252-040520402055
3. Arkawazi, A. F., Azeez, A.B., & Hamad S.M. (2020). Physical, thermal and structural properties of 1 choline chloride: 2 urea based ionic liquids. Singapore journal of scientific research,10(4),417-424. https://doi.org/10.17311/sjsres.2020.417.423
4. Barik S., Manjari C., Amita M., & Moloy S. (2022). Choline Chloride and Ethylene Glycol Based Deep Eutectic Solvent (DES) versus Hydroxyl Functionalized Room Temperature Ionic Liquids (RTILs): Assessing the Differences in the Microscopic Behavior Between DES and RTILs. Physical Chemistry Chemical Physics. 24(33). https:// 10.1039/D1CP05010A.
5. Elechi, V.U, Ikiensikimama, S.S, Akaranta, O., Ajienka, J.A & Okon, O.E. (2021). Laboratory evaluation of caricaceae plant as a locally sourced surfactant for gas hydrate inhibition in a laboratory mini flow loop. Applied Petrochemical research,11(1)295-303
6. Juric, T., Uka, D., Hollo, B. B., Jovic, B., & Kordic, B., (2021). Comprehensive physicochemical evaluation of choline chloride-based natural deep eutectic solvents. Journal of Molecular liquid, 343(3)
7. Kelland, M.A., Jana, S., Pomicpic, J., Sedlacek, O., & Hoogenboom R**.,** (2024) Kinetic Hydrate Inhibition from Thermoresponsive Poly(2-amino-2-oxazoline) s: Size and Shape of the Hydrophobic

Groups Are Critical for Performance. Energy & Fuels 38 (5),3784-3791 https://doi.org/10.1021/acs.energyfuels.3c05107

8. Khalifa, A., Ahmed, B., David, P., Roff, G., Varun, G. (2015). Inhibition effects of thermally degraded MEG on hydrate formation for gas hydrate systems. Journal of Petroleum Science and Engineering,135(4),608-617. http//doi.org/10.1016/j.petrol.2015.10.001
9. Lomba, L., Werner, Á., Giner, B., & Lafuente, C. (2023). Deep Eutectic Solvents Formed by Glycerol and Xylitol, Fructose and Sorbitol: Effect of the Different Sugars in Their Physicochemical Properties. Molecules,28(16),6023. https://doi.org/10.3390/molecules28166023
10. Lu, Y., Yuan, C., Wang, H., Yang, L., Zhang, L., Zhao, J., & Song, Y. (2022). Atomistic insights into the performance of thermodynamic inhibitors in the nucleation of methane hydrate. Chem. Eng. Journal,431(4). https://doi.org/10.1016/j.cej.2021.133479
11. Madueke C.S., Osokogwu, U., & Okon, O.O. (2023). Evaluating the performance of deep eutectic solvent using synergetic compound in gas hydrate formation. Journal of Pet and Coal,65(2) Pg353-362
12. Masri, A.N., Sulaimon, A.A. (2022). Amino acid-based ionic liquids as dual kinetic-thermodynamic methane hydrate inhibitor. Journal of molecular liquid, 349(1),118481 https://doi.org/10.1016.j.molliq.2022.118481
13. Mero, A., Koutsoumpos, S., Giannios, P., Stavrakas, I., Moutzouris, K., Mezzetta, A., & Guazzelli, L. (2023). Comparison of physicochemical and thermal properties of choline chloride and betaine-based deep eutectic solvents: The influence of hydrogen bond acceptor and hydrogen bond donor nature and their molar ratios. Journal of molecular Liquid, 377(1), 121563-121563 https://doi.org/10.1016/j.molliq.2023.121563
14. Mohammed, S.C., Jen, X. Y., & Soo, Y. L. (2021). Physicochemical properties of choline chloride – based natural deep eutectic solvent and their applicability for extracting oil palm flavonoids. Journal of molecular liquid,13(23),12981. http//doi.org/10.3390/su132312981
15. Movareji, M.K., Charffarknah, A. & Sadeghi, A. (2016). Effect of Three Representative Surfactant on Methane Hydrate Formation Rate and Induction Time. Egyptian Journal of Petroleum, 26(2),231-339.https://doi.org/10.1016/j.ejpe.2016.05.007
16. Najibi H., Azimi A., Javanmardi J., Roozbahani R., & Mohammadi, A.H. (2022). Natural gas hydrate stability conditions and water activity in aqueous solutions containing mono ethylene glycol (MEG) and salt. Fluid Phase Equilibria 554(1). https://doi/10.1016/j.fluid.2021.113322.
17. Njabulo, M., Hamed, H., & Kaniki, T. (2024). Chemical inhibitors in gas hydrate formation: A review of modelling approach Chem Engineering MDPI 8(6)
18. Nwiabu, K. Y., & Kenneth, K. D. (2018). Performances of Polyvinyl-Alcohol Inhibitor for Gas Hydrate Formation along Flow Lines. American Journal of Engineering Research,7(5)425-434
19. Odutola, T. O., & Nwisakpugi V. L. (2022). Synergistic hydrate inhibition of monoethylene glycol with polyvinyl pyrrolidone (PVP) in thermodynamic under inhibited system. Journal of Petroleum and Coal. 64(2), 221-227
20. Omar K.A., & Sadeghi R., (2022). Physicochemical properties of deep eutectic solvents: A review, Journal of Molecular Liquids, Volume 360(2),7277-7322, https://doi.org/10.1016/j.molliq.2022.119524
21. Qinze, X., Lei,W., Zhang, J., Zhang, S., & Cul, X. (2025). Experimental Study of Methane Hydrate Decomposition Kinetics in NaCl, KCl, and PVP Solutions. ACS Omega, 10(22),22647-22656.https://doi.org/10.1021/acsomega. 4c10837
22. Rao, G.L., Mandal, A., & Nilanjan, P. (2024). Choline Chloride urea based deep eutectic solvent: Characterization, interfacial behavior and synergism in binary (surfactant) system. Journal of chemical physics, 588(4),112496 https://doi.org/10.1016/j.chemphys.2024.112496
23. Scong, D.S., Hyun J.P., & Dong H.L. (2017). Effect of Poly (N-Vinyl caprolactern) molecular weight and molecular distribution on methane hydrate formation. Journal of energy and fuel,31(6),6358-6363 https://doi.org/101021/acs.energyfuels.7b00318
24. Sharma, A. & Lee B. (2024). Toxicity test profile for deep eutectic solvents: A detailed review and future prospects, Chemosphere,350(3),141097 https://doi.org/10.1016/j.chemosphere.2023.141097
25. Shen, K., Zhao, J. & Zhou, J. (2024). Experimental study on the effect of PVP, NaCl and EG on the methane hydrates formation and dissociation kinetics. Sci Rep. 14(1).16579. https://doi.org/10.1038/s41598-024-67485-w

ISSN No. 2321-2705 | DOI: 10.51244/IJRSI |Volume XII Issue X October 2025

26. Sloan, D.E & Koh, C.A. (2007). Clathrate Hydrates of Natural Gases. (3rd ed.) CRC Press https://doi.org/10.1201/9781420008494
27. Sulaiman A., Qasim, A., Athif, M., Masri, A., (2024). Phase equilibrium and kinetic studies of choline chloride-based deep eutectic solvents in water system for the inhibition of methane gas hydrate formation. Journal of Ionic Liquid.5(1),100127 https:// doi.org/10.1016/j.jil.2024.100127.
28. Syaputra, R.A., Rani, Z., Ridwanto, R., Miswanda, D. & Pulunga, A.F. (2023). Isolation and characterization of glycerol by transesterification of used cooking oil, Rasayan journal of Chemistry 16(2),648-652. https//doi.org//10.31788/RJC.2023.1628178
29. Toju, O., Uche, O., & Effiong, O. (2023). Experimental Investigation of Plant Family Extracts as Gas Hydrate Inhibitor in an Offshore Simulated Environment, Petroleum Science and Technology,42(11)1413-1430 https://doi.org/10.1080/10916466.2022.2144368